JAAS

Accepted Manuscript

This is an *Accepted Manuscript*, which has been through the Royal Society of Chemistry peer review process and has been accepted for publication.

Accepted Manuscripts are published online shortly after acceptance, before technical editing, formatting and proof reading. Using this free service, authors can make their results available to the community, in citable form, before we publish the edited article. We will replace this *Accepted Manuscript* with the edited and formatted *Advance Article* as soon as it is available.

You can find more information about *Accepted Manuscripts* in the Information for Authors.

Please note that technical editing may introduce minor changes to the text and/or graphics, which may alter content. The journal's standard Terms & Conditions and the Ethical guidelines still apply. In no event shall the Royal Society of Chemistry be held responsible for any errors or omissions in this *Accepted Manuscript* or any consequences arising from the use of any information it contains.

ROYAL SOCIETY OF CHEMISTRY

www.rsc.org/jaas

CHARACTERIZATION OF SOLID MAGNETIC NANOPARTICLES BY MEANS OF SOLID SAMPLING HIGH RESOLUTION CONTINUUM SOURCE ELECTROTHERMAL ATOMIC ABSORPTION SPECTROMETRY

E. Vereda Alonso,* M.M. López Guerrero, M.T. Siles Cordero, J.M. Cano Pavón and A. García de Torres

Magnetic nanoparticles (MNPs) are a new kind of nanometer-sized materials superparamagnetic with potential applications as magnetic carries for various biomedical uses, wastewater remediation, preconcentration of various anions and cations, etc. The excellent properties of MNPs are strongly influenced by the size of the nanoparticles. Another important factor is the amount of iron present. In this work, a simple and inexpensive approach was developed for direct determination of Fe concentration and particle size of solid MNPs by solid sampling high resolution continuum source graphite furnace atomic absorption spectrometry (HR CS GFAAS). A new strategy in evaluating area and upslope of the obtained absorbance signals for a line of Fe (352.614 nm) with low sensitivity was developed for both determinations. For this purpose, five furnace program parameters, atomization heating rate, atomization temperature, pyrolysis heating rate, pyrolysis temperature and hold pyrolysis time, were optimized with the employ of two multiple response surface designs. With the optimized furnace parameters, satisfactory calibration curves ($R \geq 0.995$) were obtained with liquid iron standards (for Fe determination) and ($R \geq 0.990$) with MNPs samples with certified size of particle (for size particle determination). The determination of the MNPs size and their percentage in iron was validated by transmission electron microscopy (TEM) and scanning electron microscopy (SEM), respectively. This method is being employed in the optimization of the synthesis of MNPs by the coprecipitation method.

1 Introduction

Nanomaterials have received a lot of attention in industry and technology due to their unique physicochemical properties. The relatively large surface area and highly active surface sites of nanoparticles enable them to have a wide range of potential applications.[1] Magnetic nanoparticles (MNPs) are a new kind of nanometer-sized superparamagnetic materials, which means that they are attracted to a magnetic field, but retain no residual magnetism after the field is removed. In recent years, MNPs have been studied because of their potential applications as magnetic carries for various biomedical uses, wastewater remediation, preconcentration of various anions and cations, etc.[2] Among MNPs, Iron oxide MNPs (magnetite, Fe_3O_4, and maghemite, ɣ-Fe_2O_3) have received the highest interest because of their biocompatibility, biodegradability, physiological and chemical stability, low toxicity and strong magnetization response.[3,4] The excellent properties of these MNPs are strongly influenced by the particle size. In the case of MNPs used in the biomedical field, the high-quality magnetic materials in terms of size affects the pharmacokinetics and the biodistribution pattern.[5] For hyperthermia applications (attractive strategy of cancer treatment based on heat generation

[1] *Department of Analytical Chemistry, Faculty of Sciences, University of Málaga*
Campus of Teatinos, 29071 Málaga, Spain. E-mail: eivereda@uma.es;
Fax: +34952132000; Tel: +34 952131883
† *Electronic supplementary information (ESI) available: TEM and SEM analysis for DPTH-MNPs and PSTH-MNPs*

on the tumor site by MNPs[6]), the heating property in the AC magnetic field is strongly influenced by the particle size;[7] MNPs sizes between 20 and 30 nm are the optimum.[8] As contrast agent in magnetic resonance imaging (MRI), small particles (< 6 nm) show reduced saturation magnetization, whereas particles > 20 nm are difficult to disperse, owing to the presence of remanent magnetization at zero field.[9]

MNPs have two main uses in analytical chemistry: separation and preconcentration of chemical species (mainly by magnetic solid-phase extraction, MSPE), and their application as sensors and biosensors.[10] Suspended superparamagnetic particles adhered to the target can be removed very quickly from a matrix using a magnetic field. this characteristic make them highly useful in separation processes. Magnetic methods have the advantages of 1) reduced analysis time, 2) they are more environmental friendly and 3) they required fewer reagents. Maghemite, for instance, has been reported for the successful removal of heavy metals such as Cr(VI)[11] and As(V)[12] from waste water. As sorbent in MSPE, they have been used in the off-line determination of trace amounts of Cr, Cu, Pb, Ag, Cd, Zn, Ni, Co, Mn in environmental samples,[1,2,4] analysis of estrogens,[13] herbicides,[14] phenolic compounds,[15] chlorophenols[16] in water samples. On-line MSPE using MNPs as sorbent is one of the latest developments. These automatic preconcentration techniques offer several important advantages over the off-line ones such as simplicity of operation, higher sample throughput, improved analytical characteristics and reduced sample and reagent consumption.[17] Automatic on-line MSPE have been described for the determination of trace amounts of Mn, Co, Cu, Zn, Pb, Cr, Pt, Pd, As, Bi, Sb, Se, Sn, Cd, Hg in environmental and biological samples[18-22], trace noble metals (Ru, Rh, Pd, Pt, Ir and Au) in geological/biological samples,[23] chromium speciation in drink waters,[24] selenium speciation in cells.[25] Iron oxide MNPs as adsorbent in MSPE have received considerable attention owning their small size and high surface area providing better kinetics and greater extraction capacity for analytes. In the case of magnetite, 16 nm seems to be the optimum size for uniform and spherical particles; for elongated Fe_3O_4, the optimum size ranges from 13 to 18 nm are also preferable because of their higher magnetic moment per particle.[8]

As noted, the properties of these MNPs are strongly influenced by the particle size; another important factor is the amount of iron or iron oxide present, in order to be properly attracted by a magnetic field. Transmission electron microscopy (TEM), scanning electron microscopy (SEM) and X-ray diffraction (XRD) are the main techniques used for the characterization and observation of the size and shape of the MNPs. The amount of iron present is usually measured by atomic absorption spectrometry (AAS) or inductively coupled plasma (ICP) spectrometry. Both methods lack the specificity to distinguish between ionic iron and nanoparticles and fail to detect the nanoparticles at low dose.[26-29] Two techniques have been reported which allow distinction of NPs from ionic species, e.g. for Ag, inductively coupled plasma mass spectrometry (ICP-MS) operating on single-particle mode[30] and graphite furnace atomic absorption spectrometry (GF-AAS), where an increase in the atomization temperature is observed with an increase in the particle size of Ag.[31] GF-AAS is more suited for complex matrices such as biological tissues, and the instrument is less expensive and more available than ICP-MS. On the other hand, both techniques required the transformation of solid samples into a liquid sample and else, in order to distinguish between particulate and soluble forms, suitable separation methods and/or data evaluation must be developed.[32,33] These methods are elaborative and time-consuming. Therefore, the development of approaches for direct investigation of solid samples omitting any sample pretreatment is

meaningful. Direct solid samples approaches can be advantageous, offering superior detection power and minimum risk of contamination since the dissolution step is avoided.[34] Solid sampling high resolution continuum source graphite furnace atomic absorption spectrometry (HR CS GFAAS) appears to be very appropriate for this objetive, because of its potential to directly analyze sub-mg samples relying on straightforward calibration with aqueous standards. The high resolution and the continuum source (HR CS), among other advantages, offers enhanced capabilities for the detection and correction of spectral interferences, as well as for expanding the linear range,[35] an aspect that becomes significant when direct solid sampling is attempted because it is not feasible to dilute the sample if the analyte content exceeds the upper limit of the linear range. In recent years, methods have been developed by HR CS GFAAS for direct analysis of nanomaterials, as the simultaneous determination of Co, Fe, Ni and Pb in carbon nanotubes,[36] or for the monitoring of nanoparticles in biological or vegetal tissues.[37,38] Moreover, Feichtmeier and Leopold,[39] have got results indicating the possibility to differentiate between nanoparticles and ion species of Ag by extracting information from their temporal signal profiles. Atomisation delays were found to be higher for samples containing silver ions than for samples containing silver nanoparticles. Furthermore, they found a correlation between the size of the Ag nanoparticles and the atomisation rates calculated as the slope of the first inflection point of the absorbance signals (upslope). Based on this last work, the objective of this study was to develop a method for direct determination of Fe concentration and particle size of solid MNPs by application of solid sampling HR CS GFAAS. A new strategy in evaluating the area and the upslope of the obtained absorbance signals for a line of Fe with low sensitivity was developed for the determination of both, iron concentration in solid MNPs and their average particle size. This method is going to be employed in the optimization of the synthesis of MNPs by the coprecipitation method.

2 Experimental

2.1. Instrumentation

An Analytik Jena ContrAA HR CS GFAAS (Analytik Jena AG, Jena, Germany), equipped with an auto sampler SSA 600 for solid sampling with integrated microbalance with a readability of 1 µg (Sartorius, Goettingen, Germany) was used in all experiments in this work. The optical system comprises a xenon short-arc lamp (GLE, Berlin, Germany) operating in “hot-spot” mode as the radiation source, a high-resolution double echelle monochromator (DEMON) and a linear CCD array detector with 588 pixels, 200 of which are used for analytical purposes (monitoring of the analytical signal and BG correction) while the rest are used for internal functions, such as correcting for fluctuations in the lamp intensity. The HR CS GFAAS instrument is also equipped with transversely heated pyrolytic graphite tubes. Solid MNPs were introduced using solid sampling graphite platforms. The typical uncertainty (standard deviation) of mass measurements (n=10) is 1 µg or lower. Data evaluation was achieved with the software ASPECT CS 2.1.2.0 (Analytik Jena AG). Atomic absorption of iron was detected at 352.614 nm, which is an iron line with low sensitivity. The temperature program for the graphite furnace used for the determination of iron concentration and nanoparticle size is given in Table 1.

For validation purpose, the size and Fe concentration, in percentage, of the MNPs were also determined by transmission electron microscopy (TEM, JEOL, JEM-1400) and scanning electron microscopy (SEM, JEOL, JFM 840) operated at 20 KV.

2.2. Reagents and samples

High purity reagents were used in all experiments. Doubly de-ionized water (18 MΩ cm) was obtained from a milli-Q water system (Millipore, Bedford, MA, USA). A standard of 10,000 mg L^{-1} for Fe(II) solution (Sigma Aldrich, St. Louis, USA) was used. Standards of working strength were made immediately prior to use. 1,000 mg L^{-1} Pd chemical modifier solution (Sigma Aldrich, St. Louis, USA) was also used. As calibration standards for size determinations, Iron Oxide(II,III) magnetic nanopowder 5±1 and 30±2 nm diameter, N-Hydroxysulfosuccinimide functionalized were purchased from Sigma-Aldrich (St. Louis, USA) and Iron Oxide (II,III) nanopowder/nanoparticle (Fe_3O_4, high purity, 99.5+%, 15-20 nm) was purchased from US Research Nanomaterials, Inc. (Houston, USA). Two previously synthesized by us silica-coated magnetic nanoparticles modified with [1,5-bis(2-pyridyl)-3-sulphophenyl methylene] thiocarbonohydrazide (PSTH-MNPs) and with 1,5-bis(di-2-pyridil)methylene thiocarbohydrazide (DPTH-MNPs)[21,22] were employed for the optimization of the procedure. These samples were also analyzed by TEM and SEM. The average size of the nanoparticles of the standard from US Research Nanomaterials, Inc., was also determined by TEM, resulting in an average size of 17±2 nm.

2.3. Optimization strategy

Five furnace program parameters were optimized with the use of two multiple response surface designs. The response functions chosen were: atomization signal area/weighted mass of MNPs and the inverse of the upslope of the atomization signal/weighted mass of MNPs; in order to obtain atomization signals with high areas and smoothed slopes that can increase with the MNPs size. The signals are divided by the mass due to dificulty to weigh the same sample amount everytime. The measurement of the slope was realized by using Microsoft Excell software. First, the first derivative of the atomization curve was realized and the first inflexion point localized, then the slope in the straight section around this point was calculated (Figure 1). Two rotatable uniform central composite designs were performed. The lower and upper values of the factors are given in Table 2. A sample mass, ca 0.10 mg of DPTH-MNPs was selected to perform the optimization.

The designs used included a total of $2^k + 2k + n$ runs, where k is the number of studied parameters (k = 3 in the first design and k = 2 in the second), 2^k are the points from the factorial experiments carried out at the corners of the cube and $2k$ are the points carried out on the face centered star. The repetition of the center point was used to estimate the experimental error (n = 2, in both design). The resulting 16 and 10 experiments for the first and second design, respectively, were randomly performed.

The experimental data were processed by using the STATGRAPHICS Centurion XVI. For the designs, the significance of the effects was checked by analysis of the variance (ANOVA) and using p-value significance levels. This value represents the probability of the effect of a factor being solely due to the random error. Thus, if the p-value is less than 5%, the effect of the corresponding factor is significant.

2.4. Procedure for analysis by solid sampling with HR CS GFAAS

Samples were directly analyzed without any prior preparation step. The solid sampling device used allows for automatic weighing and transporting of the samples into the furnace. The platform was first transported to the microbalance using a pair of tweezers. After taring, an appropriate amount of the sample (between 0.05 and 2.00 mg) was placed on the platform and weighed. A 5-20 µL volume of a 1000 mg L^{-1} Pd chemical modifier solution was dosed onto the sample and the platform was transferred to the graphite furnace and subjected to the temperature program (Table 1). All operations were fully controlled by the computer, except for the deposition of the sample and the modifier solutions onto the platform, which were manually undertaken. Integrated absorbance was selected as the measurement mode for the determination of iron concentration. For the atomic line evaluated, the absorbance values obtained at each of three detector pixels (the central pixel plus the adjacent ones, CP ± 1) were summed. The slope on the first inflexion point of the atomization signal (upslope) was also measured as described above for the determination of the MNPs average size.

For the determination of iron concentration, external calibration was performed by using variable volumes (5, 10, 15 and 20 µL) of 5,000 mg L^{-1} iron standard dosed with a micropipette onto the sampling platform together with the modifier solution. Other external calibration was performed using the standards from Sigma-Aldrich and US Research Nanomaterials, Inc described in *2.2. Reagents and samples*. Due to the iron concentration of 5 and 30 nm standards (Sigma-Aldrich) was significantly lower than the iron concentration of the 17 nm standard (US Research Nanomaterials, Inc) and the iron concentration of the samples DPTH-MNPS and PSTH-MNPs, approximately 2 mg of 5 and 30 nm standards had to be weighted, in order to obtain similar atomization signals; then 20 µL volume of chemical modifier solution was dosed for this two standards. The ratio between the slope of the atomization signal on the first inflexion point (calculated through the slope function of Microsoft Excell software, figure 1) and the peak area (which is directly proportional to the amount of Fe in the standard) was used as measurement parameter for the average size MNPs determination.

Three replicate measurements were made for liquid iron standards and five replicate measurements (representing approximately 10-15 minutes of work) were made for each solid measurement in order to improve the precision[40].

3 Results and discussion

3.1. Wavelength selection

As noted earlier, the goal of this work was to develop a method for the direct determination of iron concentration and particle size of solid MNPs. The iron concentration in this type of materials is high (%, w/w). An important aspect in the direct analysis of solid samples is to achieve the determination of the analyte without the dilution of the sample; so a line with very low sensitivity must be chosen. The line at 352.604 nm has a relative sensitivity respect to the most sensitive line for Fe of 0.11 %. At this wavelentgh, iron presents a duplet (352.604/352.614 nm)[41], with m_0 of 3 and 27 ng, respectively, the line at 352.614 nm is much

less sensitive, which is fit for purpose in this case. The spectrum of a DPTH-MNPs sample is shown in Figure 2.

One of the main characteristics of HR CS GFAAS instrument is its excellent resolution, with a CCD detector comprising 588 pixels, of which 200 are used for analytical purposes while the rest are used for internal corrections. Each pixel monitors a range of only 1 to 2 pm (the exact value depends on wavelength: the lower the wavelength, the higher the resolution). As was mentioned above, for the atomic line evaluated, the absorbance values obtained at each of three detector pixels (the central pixel plus the adjacent ones, CP ± 1) were summed.

3.2. Pyrolysis and atomization conditions

Once the appropiate wavelentgh was selected, optimal conditions for direct analysis of MNPs were investigated using the functionalized MNPs synthesized by us, DPTH-MNPs. Despite having selected a low sensitive line, the iron concentration in this samples is very high, about of 60% w/w. Thus, in order to obtain appropiate atomization peaks, a sample mass of about 0.10 mg was chosen to perform the optimzation. Based on the paper by Resano et al,[41] in which iron was determined at the selected wavelength in this work, 5 µg Pd (added as $Pd(NO_3)_2$) was used as modifier, and the furnace program parameters described in this paper were used as a starting point for the optimization. Pyrolysis and atomization steps are the most critical factors in order to remove most matrix component without analyte losses and obtain well defined atomization peaks for the solid samples. A fruitful way to adjust some variables in order to establish optima measurement conditions is the surface-response methodology (SRM). This includes a group of mathematical-statistical techniques that were designed to optimize the analytical response by producing a model in which a response function corresponds to several variables called factors. Five factors were optimized following this methodology: pyrolysis and atomization temperatures (°C), pyrolysis and atomization ramps (°C s^{-1}) and pyrolysis hold time (s). The aim of this work was to determine the iron concentration and the average particle size of MNPs. As was mentioned by Feichtmeier and Leopold[39] for Ag nanoparticles, in preliminary experiments we found similar correlations between the size of the MNPs and the slope on the first inflection point of the absorbance signals. So, two response functions were chosen to maximize in the SRM: atomization signal area/weighted mass of MNPs and the inverse of the upslope of the atomization signal/weighted mass of MNPs. This selection was done in order to obtain (independently of the MNPs weighted mass, normalized) adequate peak areas for the determination of iron, and atomization peaks with smoother upslopes to distinguish between the upslopes due to MNPs of different sizes. Multiple response (two response functions) rotatable uniform central composite designs were performed. The lower and upper values given to the factors are given in Table 2. The three dimensional representations of the both designs are presented in Figure 3A and 3B , respectively. These figures show the combination of factors to which the optimum is reached. The values of these factors are given in Table 1.

3.3. Calibration strategy

Iron concentration

Once optimum conditions were established, the posibility to quantitate using calibration against aqueous standards was explored. As can be seen in figure 1, unimodal well-defined signal profiles were obtained for iron, even for direct solid MNPs sampling. Moreover, no indication of spectral overlap was observed, and a stable baseline was attained. Although dissimilar signal profiles were obtained for aqueous and solid samples, both provided complete atomization (Figure 4). So using integrated peak areas makes it feasible to calibrate with aqueous standards.[35] In fact, comparable sensitivities were obtained for solid MNPs and aqueous iron standards. Therefore, analysis of the samples can be achieved using calibration curves constructed with aqueous standards Figure 5A.

Average size of MNPs

The great problem found to stablish a calibration strategy was to find adequate MNPs with certified average size for their use as standards. In a first moment, we found, N-Hydroxysulfosuccinimide functionalized iron Oxide(II,III) magnetic nanopowder 5 and 30 nm diameter, commercialized by Sigma-Aldrich and no functionalized iron Oxide(II,III) magnetic nanopowder of high purity (99.5+%) 15-20 nm, commercialized by US Research Nanomaterials, Inc. Then, a calibration curve based on the normalized upslope (dividing by the weighted mass) was tried with the optimum conditions studied. However, due to the different iron concentrations of the standards, the atomization signals were no comparable. The iron concentration in the standards by Sigma-Aldrich is around 1.4% w/w whereas the iron concentration in the standard by US Research Nanomaterials, Inc., found by us, was 70±3% w/w.

In order to obtain comparable atomization signals, different masses were weighted depending of the iron concentration in the standard, and the upslopes obtained were normalized dividing by the Fe mass (g) calculated from the weighted mass of standard and its iron concentration. Different sample masses require different furnace temperature conditions, besides, the 30 nm standard from Sigma-Aldrich resulted to be very hygroscopic. So, given the high price of the Sigma-Aldrich size standard MNPs, and to avoid having to change the pyrolysis and atomization conditions, we opted for working with small amounts of MNPs, between 0.05 mg (the measurable minimum weight by the balance is 0.02 mg) and 2.00 mg. The 30 nm standard from Sigma-Aldrich was used to optimize the drying conditions and the amount of modifier to use with higher amounts of MNPs.

Tests were made with and without modifier; the results obtained without modifier were unsatisfactory, even the upslopes appeared to decrease with the size of the MNPs instead of increasing. In theory, larger MNPs (assembly of several 100 iron atoms) produce more free atoms at a time, so higher upslopes should be obtained. On this way, the modifier volume was studied for 1 mg of 30 nm standard. It was observed that when 1 mg of MNPs was used, higher volume of modifier was necessary. Finally, 20 µL of modifier ($Pd(NO_3)_2$ 1000 mg L^{-1}) were added. With this volume it was observed that the total amount weighed of MNPs was moisturized with the modifier. The Analytik Jena ContrAA HR CS GFAAS is equipped with an optical camera to observe the drying of the samples. A complete drying of the 30 nm standard was observed with a drying ramp time of 10 °C s^{-1} and a hold time of 90 s.

With these new conditions, a calibration graph was built by representing the normalized (dividing by Fe mass) slope on the first inflexion point of the atomization signal (Figure 1) versus average size of MNPs standards supplied by Sigma-Aldrich and US Research Nanomaterials, Inc. The relative standard deviations obtained for the standards were high (>10%, RSD). On the other hand, if the peak area is proportional to the Fe amount in the samples, the division by the peak area would be better than the division by the Fe amount; besides the method would be simpler, because the calculation of the concentration of iron would be unnecessary to determine the size of the nanoparticles. On this way, the reproducibility of the results was improved. %RSDs were calculated for five replicates of the three standards, the obtained values were 4.1, 7.3 and 3.5 % for 5, 17, and 30 nm, respectively. Thus, the average RSD of the method in this size range is around 5%. The calibration graph obtained is shown in Figure 4B.

3.4. Applications

The method was applied to the determination of Fe concentration and average particle size of two previously synthesized by us functionalized magnetic nanoparticles, DPTH-MNPs and PSTH-MNPs. The atomization signal of these materials were very similar in shape and in peak area values to those of MNPs used for calibration. The atomization signal of DPTH-MNPs is shown in Figure 4. The results found are shown in Table 3. Three replicates were employed for aqueous standards and five replicates were used for both, solid standards and samples. The results obtained for iron concentration and average size were well compared with those obtained by SEM and TEM, or indicated in the especification sheets provided by Sigma-Aldrich of the calibration standards for size determinations. As ESI† can be seen TEM and SEM analysis for DPTH-MNPs and PSTH-MNPs. In order to test the applicability of the method, unfunctionalized MNPs were synthesized in different conditions in order to obtain different sizes. The results of the analysis of these samples are shown in Table 4. As can be seen, MNPs with higher iron concentration are larger.

Conclusions

In this work, a simple and inexpensive approach was developed for direct determination of Fe concentration and particle size of solid MNPs by solid sampling HR CS GFAAS. The furnace program was optimized by means two multiple response (two response) multivariate experimental desings. A new strategy in evaluating area and slope on the first inflexion point of the atomization signal was developed. The principal problem found was to obtain MNPs as size standards. Very few MNPs samples, functionalized or no, can be found on trade with certified particle size; and the iron concentration in these samples is very different. So, the upslope was normalized dividing by the peak area, which is directly proportional to the iron amount weighed. There are other techniques that can provide this type of information, but most of them require performing some sample pretreatment (e.g. dissolution) which always represents a serious risk, as it is hard to preserve the exact way in which the analyte is present throughout this process. However, with solid sampling HR CS GFAAS, these determinations can be made directly to solid sampling.

The method was succesfully validated by TEM and SEM analysis of two previously sinthesized by us functionalized silica-coated MNPs, DPTH-MNPs and PSTH-MNPs. This method is being employed in the optimization of the synthesis of MNPs by the coprecipitation method, in order to obtain MNPs with high iron concentrations and small size to be used as adsorbent in solid phase microextraction procedures. Small sized MNPs with high iron concentration are preferable because their higher surface area and higher magnetic moment per particle. Higher surface area provides better kinetics and greater extraction capacity for analytes, while higher magnetic moment per particle provides better attraction by a magnet for the purpose of being retained in a reactor.

Acknowledgements

The authors thank the Spanish Ministerio de Ciencia y Tecnología (MCyT project no. CTQ2013-44791-P) for supporting this study and also FEDER funds.

References

1 J.S. Suleiman, B. Hu, H. Peng, C. Huang, *Talanta,* 2009, **77**, 1579.
2 M.H. Mashhadizadeh, Z. Karami, *J. Hazard Mater*., 2011, **190**, 1023.
3 J.E. Kim, J.Y. Shin, M.H. Cho, *Arch. Toxicol.,* 2012, **86**, 685.
4 A.E. Karatapanis, Y. Fiamegos, C.D. Stalikas, *Talanta*, 2011, **84**, 834.
5 L. Gutiérrez, R. Costo, C. Grüttner, F. Westphal, N. Gehrke, D. Heinke, A. Fornara, Q.A. Pankhurst, C. Johansson, S. Veintemillas-Verdaguer, M.P. Morales, *Dalton Trans.,* 2015, **44**, 2943.
6 C.S.S.R. Kumar, F. Mohammad, *Adv. Drug Delivery Rev.,* 2011, **63**, 789.
7 H. Aono, H. Hirazawa, T. Naohara, T. Maehara, H. Kikkawa, Y. Watanabe, *Mater. Res. Bull.,* 2005, **40**, 1126.
8 M. Marciello, V. Connord, S. Veintemillas-Verdaguer, M.A. Vergés, J. Carrey, M. Respaud, C.J. Serna, M. P. Morales, *J. Mater. Chem. B,* 2013, **1**, 5995.
9 A. Ruiz, G. Salas, M. Calero, Y. Hernández, A. Villanueva, F. Herranz, S. Veintemilllas-Verdaguer, E. Martínez, D.F. Barber, M.P. Morales, *Acta Biomater.,* 2013, **9**, 6421.
10 K. Aguilar-Arteaga, J.A. Rodríguez, E. Barrado, *Anal. Chim. Acta,* 2010, **674**, 157.
11 J. Hu, G. Chem, L.M.C. Lo, *Water Res*., 2005, **39**, 4528.
12 T. Tuutijrvi, J. Lu, M. Sillanpä ä, G. Chen, *J. Hazard. Mater.,* 2009, **166**, 1415.
13 Y. Liu, L. Jia, *Microchem. J.,* 2008, **89**, 72.
14 Y. Song, S. Zhao, P. Tchounwou, Y-M. Liu, *J. Chromatogr. A,* 2007, **1166**, 79.
15 X. Zhao, Y. Shi, T. Wang, Y. Cai, G. Jiang, *J. Chromatogr. A,* 2008, **1188**, 140.
16 J. Li, X. Zhao, Y. Shi, Y. Cai, S. Mou, G. Jiang, *J. Chromatogr. A,* 2008, **1180**, 24.
17 G. Giakisikli, A.N. Anthemidis, *Anal. Chim. Acta,* 2013, **789**, 1.
18 P-L. Lee, Y-C. Sun, Y-C. Ling, *J. Anal. At. Spectrom.,* 2009, **24**, 320.
19 Y. Wang, X. Luo, J. Tang, X. Hu, Q. Xu, C. Yang, *Anal. Chim. Acta,* 2012, **713**, 92.
20 B. Chen, S. Heng, H. Peng, B. Hu, X. Yu, Z. Zhang, D. Pang, X. Yue, Y. Zhu, *J. Anal. At. Spectrom.,* 2010, **25**, 1931.
21 E. Vereda Alonso, M.M. López Guerrero, P. Colorado Cueto, J. Barreno Benítez, J.M. Cano Pavón, A. García de Torres, *Talanta,* 2016, **153**, 228.

22 M. M. López Guerrero, E. Vereda Alonso, J. M. Cano Pavón, M. T. Siles Cordero and A. García de Torres, *J. Anal. At. Spectrom.,* 2016, **31**, 975.
23 Y. Li, Y-F. Huang, Y. Jiang, B-I. Tian, F. Han, X-P. Yan, *Anal. Chim. Acta,* 2011, **692**, 42.
24 Y.F. Huang, Y. Jiang, X-P. Yan, *J. Anal At. Spectrom.,* 2010, **25**, 1467.
25 B. Chen, B. Hu, M. He, Q. Huang, Y. Zhang, X. Zhang, *J. Anal. At. Spectrom.,* 2013, **28**, 334.
26 J. Dong, Z. Xu, F. Wang, *Appl. Surf. Sci.,* 2008, **254**, 3522.
27 C.R. Valois, J.M. Braz, E.S. Nunes, M.A. Vinolo, E.C. Lima, R. Curi, W.M. Kuebler, R.B. Azevedo, *Biomaterials.* 2010, **31**, 366.
28 S. Arora, J.M. Rajwade, K.M. Paknikar, *Toxicol. Appl. Pharmacol.,* 2012, **258**, 151.
29 A. Ruiz, Y. Hernández, C. Cabal, E. Gonzáles, S. Veintemillas-Verdaguer, E. Martínez, M.P. Morales, *Nanoscale,* 2013, **5**, 11400.
30 D.M. Mitrano, E.K. Lesher, A. Bednar, J. Monserud, C.P. Higgins, J.F. Ranville, *Environ. Toxicol. Chem.,* 2012, **31**, 115.
31 F. Gagné, P. Turcotte, C. Gagnon, *Anal. Bioanal. Chem.,* 2012, **404**, 2067.
32 K. Loeschner, J. Navratilova, C. Købler, K. Mølhave, S. Wagner, F. von der Kammer, E.H. Larsen, *Anal. Bioanal. Chem.,* 2013, **405**, 8185.
33 J-B. Chao, J-F. Liu, S-J. Yu, Y-D. Feng, Z-Q. Tan, R. Liu, Y-G. Yin, *Anal. Chem.,* 2011, **83**, 6875.
34 E. Muñoz-Delgado, J-C-Morote-García, R. Romero-Romero, I. López-García, M. Hernández-Córdoba, *Anal. Biochem.,* 2006, **348**, 64.
35 M. Resano, M. Aramendia, M.A. Belarra, *J. Anal. At. Spectrom.,* 2014, **29**, 2229.
36 M. Resano, E. Bolea-Fernández, E. Mozas, M.R. Florez, P. Grinberg, R.E. Sturgeon, *J. Anal. At. Spectrom.,* 2013, **28**, 657.
37 M. Resano, E. Mozas, C. Crespo, J. Briceño, J. del Campo Menoyo, M.A. Belarra, *J. Anal. At. Spectrom.,* 2010, **25**, 1864.
38 M. Resano, A.C. Lapeña, M.A. Belarra, *Anal. Methods,* 2013, **5**, 1130.
39 N.S. Feichtmeier, K. Leopold, *Anal. Bioanal. Chem.,* 2014, **406**, 3887.
40 M.A. Belarra, M. Resano, J.R. Castillo, *J. Anal. At. Spectrom.,* 1999, **14**, 547.
41 M. Resano, L. Rello, M. Flórez, M.A. Belarra, *Spectrochim. Acta Part B,* 2011, **66**, 321.

Table 1. Optimized furnace program

Step	Temperature/°C	Ramp time/°C s^{-1}	Hold time/s
Drying	150	10	90
Pyrolysis	1050	75	5
Auto-zero	1050	0	5
Atomization	2500	1275	12
Cleaning	2600	500	4

Table 2. Lower and upper values for Central Composite Desings

	First Desing		
Step	Pyrolysis Temperature/°C	Atomization Ramp/°C s^{-1}	Atomization Temperature/°C
Min	800	1000	2300
Max	1300	1500	2600
	Second Desing		
Step	Pyrolysis Ramp/°C s^{-1}	Pyrolysis Hold/s	
Min	30	10	
Max	100	60	

Table 3. Results of the determination of the iron concentration and average size of MNPs

SS-CS-GFAAS			SEM	TEM
Sample	[Fe] (%)	Average Size (nm)	[Fe] (%)	Average Size (nm)
DPTH-MNPs	57±6	14±4	57.5	13±2
PSTH-MNPs	61±1	13±2	65.6	13±1
5 nm standard	1.49±0.14		--	5±1[b]
30 nm standard	1.3±0.3		1.25[a]	30±2[b]
15-20 nm standard	70±3		72[c]	17±2

[a,b] Data obtained from the specification sheet by Sigma-Aldrich

[b] Average size informed by Sigma-Aldrich was obtained by means TEM

[c] Calculated from its purity (99.5%) and molecular formula, Fe_3O_4

Table 4. Applications

Sample	[Fe] (%)	Average Size (nm)
MNPs 1	75±3	20±1
MNPs 2	82±2	21,9±0,7
MNPs 3	65±6	16±2

Figure 1. Atomization signals for 5, 17 and 30 nm MNPs standards. The measurement of the slope was realized by using Microsoft Excell software.

Figure 2. Spectrum of DPTH-MNPs.

Figure 3. Results of the CCD designs.

Figure 4. (A) Atomization signal for an iron liquid standard standard.

(B) Atomization signal for functionalized silica coated MNPs (DPTH-MNPs).

Figure 5. (A) Calibration graph for [Fe], constructed with aqueous standards.

(B) Calibration graph for MNPs size determination.

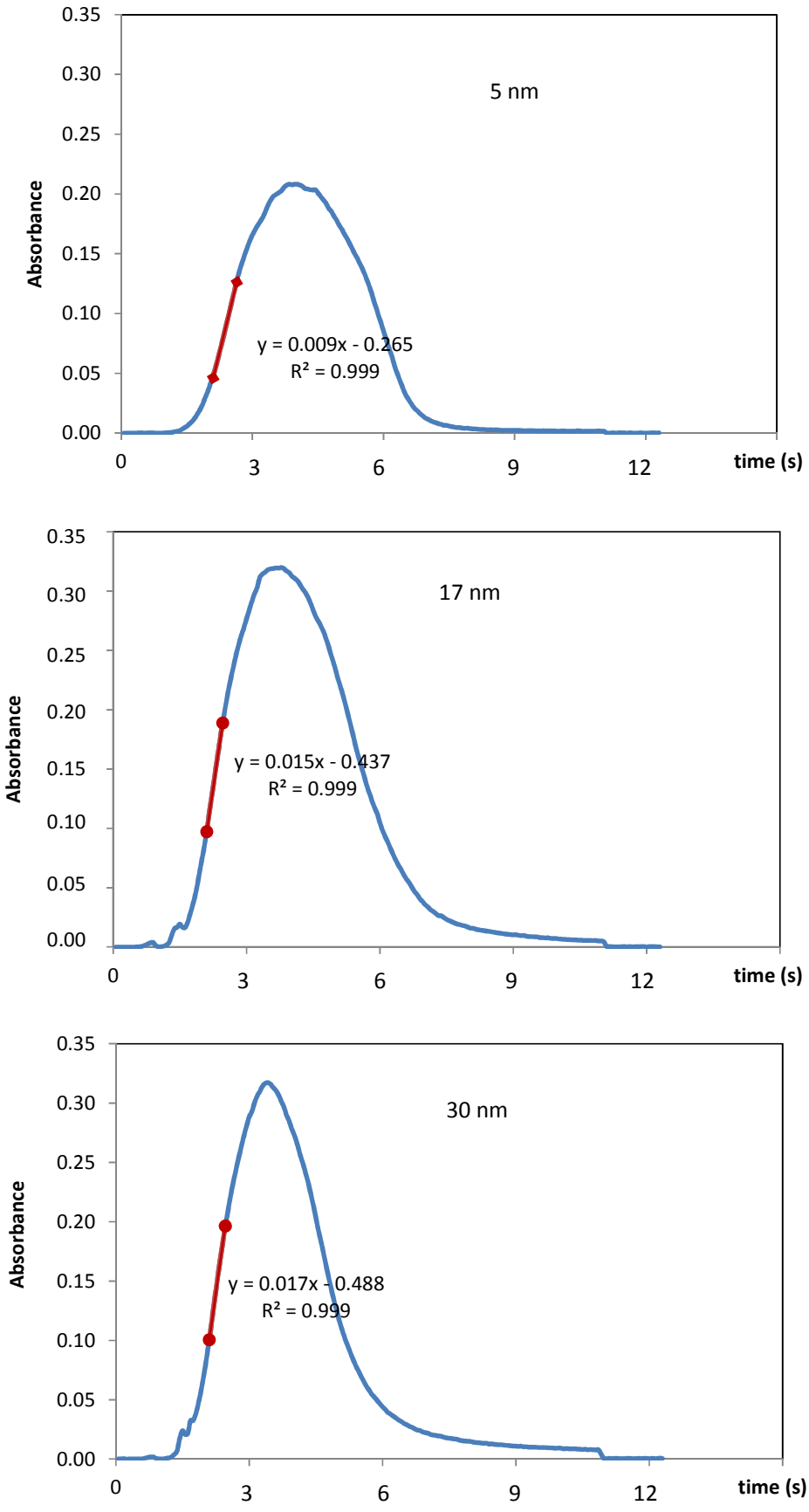

Figure 1

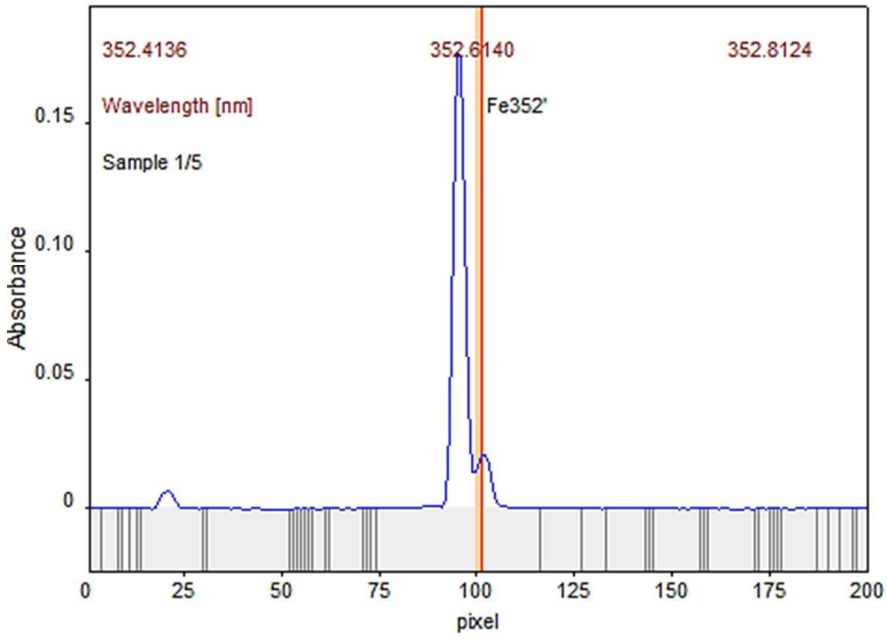

Figure 2

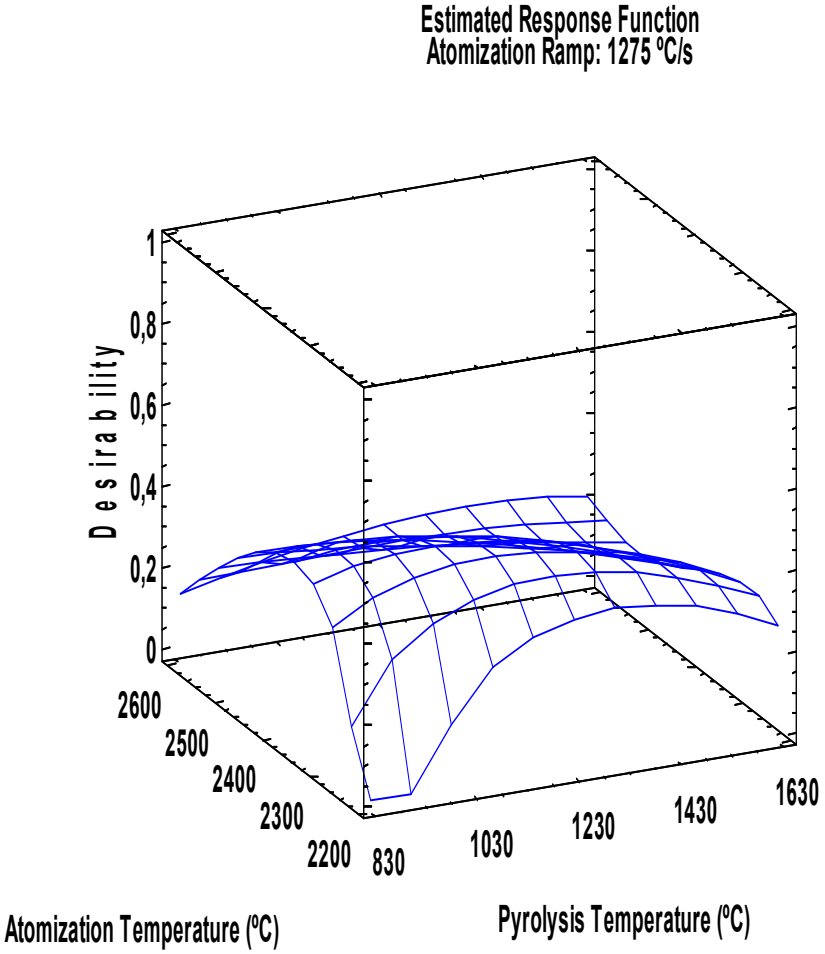

(A)

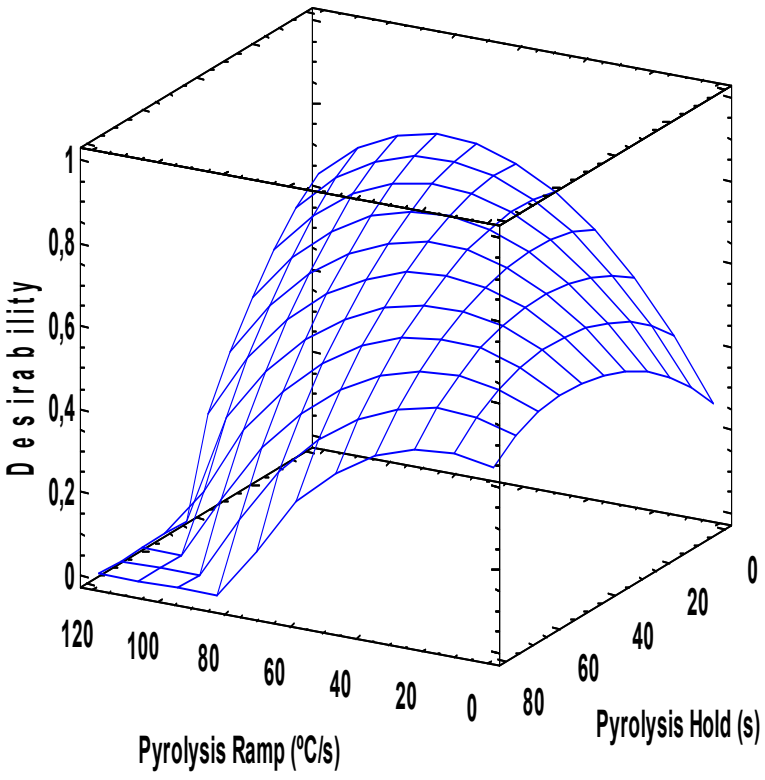

(B)

Figure 3

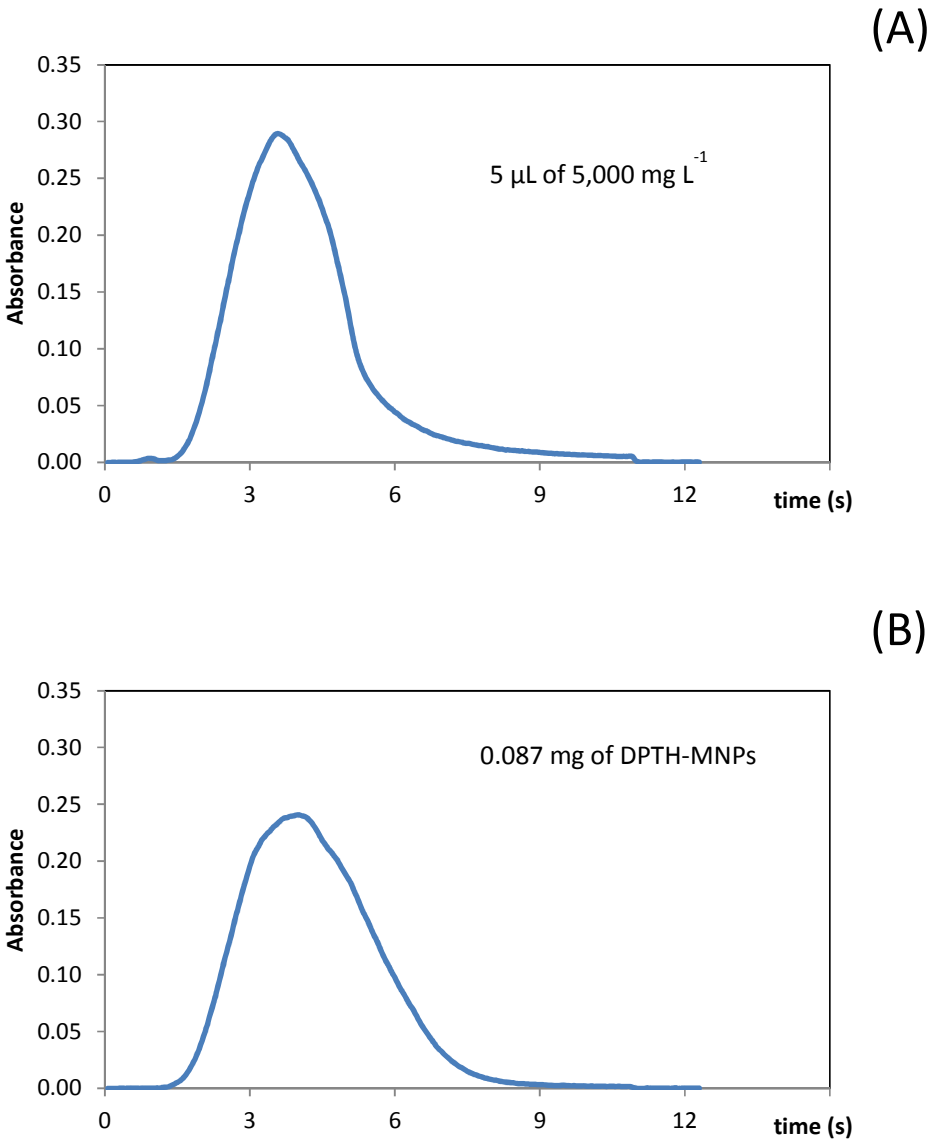

Figure 4

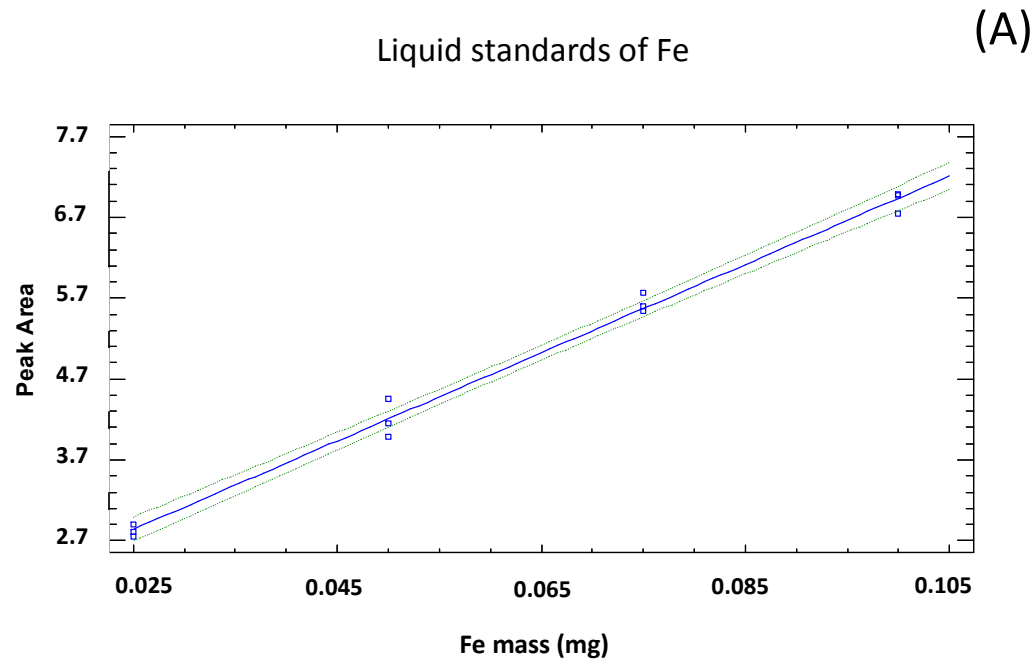

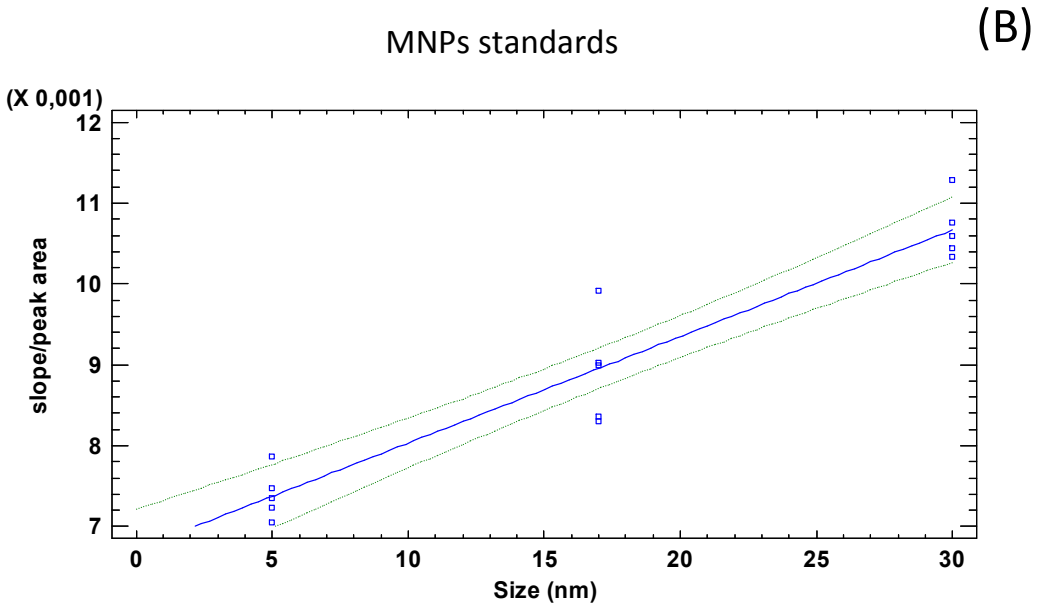

Figure 5